

# UC San Diego

## UC San Diego Previously Published Works

### Title

Longitudinal Trajectories of Regional Cerebral Blood Flow in Very Preterm Infants during Third Trimester Ex Utero Development Assessed with MRI

### Permalink

<https://escholarship.org/uc/item/2tk6n55w>

### Journal

Radiology, 299(3)

### ISSN

0033-8419

### Authors

Zun, Zungho  
Kapse, Kushal  
Jacobs, Marni  
[et al.](#)

### Publication Date

2021-06-01

### DOI

10.1148/radiol.2021202423

Peer reviewed


# Longitudinal Trajectories of Regional Cerebral Blood Flow in Very Preterm Infants during Third Trimester ex Utero Development Assessed with MRI

Zungho Zun, PhD • Kushal Kapse, MS • Marni Jacobs, PhD • Sudepta Basu, MD • Mariam Said, MD • Nicole Andersen, BA • Jonathan Murnick, MD • Taeun Chang, MD • Adre du Plessis, MBChB • Catherine Limperopoulos, PhD

From the Division of Diagnostic Imaging and Radiology, Children's National Hospital, 111 Michigan Ave NW, Washington, DC 20010 (Z.Z., K.K., N.A., J.M., C.L.); Division of Fetal and Transitional Medicine, Children's National Hospital, Washington, DC (Z.Z., A.d.P., C.L.); Departments of Pediatrics (Z.Z., M.J., S.B., M.S., J.M., T.C., A.d.P., C.L.) and Radiology (Z.Z., J.M., C.L.) and Divisions of Neonatology (S.B., M.S.) and Neurology (T.C.), Children's National Hospital, George Washington University School of Medicine and Health Sciences, Washington, DC; Division of Biostatistics and Study Methodology, Children's National Research Institute, Washington, DC (M.J.). Received May 26, 2020; revision requested August 6; revision received January 15, 2021; accepted February 5. **Address correspondence to** C.L. (e-mail: [CLimpero@childrensnational.org](mailto:CLimpero@childrensnational.org)).

Supported by the National Institutes of Health (grants U54HD090257, R01HL116585, R01HD099393, and R01HD100012).

Conflicts of interest are listed at the end of this article.

Radiology 2021; 299:691–702 • <https://doi.org/10.1148/radiol.2021202423> • Content codes:  

**Background:** The third trimester of gestation is a crucial phase of rapid brain development, but little has been reported on the trajectories of cerebral blood flow (CBF) in preterm infants in this period.

**Purpose:** To quantify regional CBF in very preterm infants longitudinally across the ex utero third trimester and to determine its relationship with clinical factors associated with brain injury and premature birth.

**Materials and Methods:** In this prospective study, very preterm infants were enrolled for three longitudinal MRI scans, and 22 healthy full-term infants were enrolled for one term MRI scan between November 2016 and February 2019. Global and regional CBF in the cortical gray matter, white matter, deep gray matter, and cerebellum were measured using arterial spin labeling with postlabeling delay of 2025 msec at 1.5 T and 3.0 T. Brain injury and clinical risk factors in preterm infants were investigated to determine associations with CBF. Generalized estimating equations were used to account for correlations between repeated measures in the same individual.

**Results:** A total of 75 preterm infants (mean postmenstrual age [PMA]: 29.5 weeks  $\pm$  2.3 [standard deviation], 34.9 weeks  $\pm$  0.8, and 39.3 weeks  $\pm$  2.0 for each scan; 43 male infants) and 22 full-term infants (mean PMA, 42.1 weeks  $\pm$  2.0; 13 male infants) were evaluated. In preterm infants, global CBF was 11.9 mL/100 g/min  $\pm$  0.2 (standard error). All regional CBF increased significantly with advancing PMA ( $P \leq .02$ ); the cerebellum demonstrated the most rapid CBF increase and the highest mean CBF. Lower CBF was associated with intraventricular hemorrhage in all regions ( $P \leq .05$ ) and with medically managed patent ductus arteriosus in the white matter and deep gray matter ( $P = .03$ ). Mean CBF of preterm infants at term-equivalent age was significantly higher compared with full-term infants ( $P \leq .02$ ).

**Conclusion:** Regional cerebral blood flow increased significantly in preterm infants developing in an extrauterine environment across the third trimester and was associated with intraventricular hemorrhage and patent ductus arteriosus.

© RSNA, 2021

Online supplemental material is available for this article.

Neurodevelopmental disabilities after premature exposure to extrauterine life remain prevalent and manifold and include motor, cognitive, behavioral, and socioaffective impairments (1). Notably, these neurodevelopmental impairments often take years to manifest, and early biomarkers of risk are needed to guide medical and rehabilitative interventions that mitigate risk.

Coincident with premature extrauterine exposure are critical periods of brain development that may place the preterm infant at risk for impaired brain development. Third trimester brain development is particularly accelerated (2,3), presumably because of energy-dependent processes that demand an increasing supply of blood-borne oxygen and nutrients to the brain. Until recently, our ability to safely measure and monitor the developmental

trajectories of regional cerebral blood flow (CBF) in the ex utero preterm infant over the third trimester of development was limited.

Arterial spin labeling (ASL) has emerged as a powerful MRI tool to use in the quantitative measurement of regional CBF, as there is no contrast agent or exposure to ionizing radiation (4,5). Several prior studies have used ASL to study CBF in preterm infants, but ASL has largely been used at term-equivalent age (TEA) or in studies with a cross-sectional design (6–15). Longitudinal noninvasive assessment of CBF in different regions of the immature brain during the ex utero third trimester will allow better understanding of the role of premature exposure to the extrauterine milieu and its association with brain injury and clinical risk factors.

## Abbreviations

ASL = arterial spin labeling, CBF = cerebral blood flow, CGM = cortical gray matter, DGM = deep gray matter, IVH = intraventricular hemorrhage, PDA = patent ductus arteriosus, PMA = postmenstrual age, TEA = term-equivalent age, WM = white matter

## Summary

Regional cerebral blood flow in preterm infants increased with advancing postmenstrual age during the third trimester and was lower in infants with intraventricular hemorrhage and medically managed patent ductus arteriosus.

## Key Results

- Mean cerebral blood flow (CBF) in preterm infants increased significantly with advancing postmenstrual age in all regions during the third trimester ( $P \leq .02$ ).
- The cerebellum demonstrated the most rapid increase in CBF and the highest mean CBF.
- Lower CBF was associated with intraventricular hemorrhage in all regions ( $P \leq .05$ ) and with medically managed patent ductus arteriosus in white matter and deep gray matter ( $P = .03$ ).

Our study objectives were twofold: (a) to examine temporal changes of global and regional CBF in preterm infants over the third trimester of ex utero development and (b) to examine the relationship of CBF with clinical factors associated with brain injury and premature birth.

## Materials and Methods

### Study Population

This prospective study was compliant with the Health Insurance Portability and Accountability Act and was approved by the institutional review board of Children's National Hospital. Written informed consent was obtained from the parents of each infant. Seventy-eight very preterm infants and 27 healthy full-term infants without a clinical indication for MRI were consecutively enrolled between November 2016 and February 2019. Inclusion criteria for preterm infants were gestational age of 32 weeks or less at birth and birth weight of 1500 g or less. Inclusion criteria for full-term infants were normal prenatal history, normal screening laboratory results, and normal US findings in the brain. Exclusion criteria for both preterm and full-term infants included chromosomal anomalies, congenital malformations, central nervous system infection, and metabolic disorders.

### Imaging Protocol

Enrolled preterm infants underwent three MRI examinations (referred to as MRI 1, MRI 2, and MRI 3 hereafter), with target study times of 1–2 weeks of life for MRI 1, 34–36 weeks of postmenstrual age (PMA) for MRI 2, and 37–42 weeks of PMA (ie, TEA) for MRI 3. Healthy full-term infants underwent one MRI scan in the newborn period. All MRI 1 studies and the majority of MRI 2 examinations of preterm infants were performed with a 1.5-T GE MR450 scanner (GE Healthcare). A few MRI 2 (eight of 67) and all MRI 3 scans of preterm infants, as well as all full-term MRI scans, were performed with a 3.0-T GE MR750 scanner (GE Healthcare). Infants were examined during

natural sleep using the feed and bundle approach, without sedation unless clinically indicated. For CBF measurement, ASL was performed using a three-dimensional pseudocontinuous ASL scheme (16) with the following imaging parameters: repetition time msec/echo time msec, 4700–4900/11; field of view, 12–16 cm; in-plane resolution, 2.7–3.5 mm<sup>3</sup>; section thickness, 3–4 mm<sup>3</sup>; number of sections, 22–36; postlabeling delay, 2025 msec (determined based on an ASL consensus report [25]); labeling duration, 1450 msec; and scan time, approximately 5 minutes. This ASL protocol was consistent for all scans performed at both field strengths. For T2-weighted anatomic imaging, either a three-dimensional fast spin-echo or a two-dimensional single-shot fast spin-echo sequence was performed. Total scanning time of each examination, including other sequences in our protocol (eg, spectroscopy, diffusion, and functional MRI), was approximately 1 hour.

### CBF Quantification

CBF quantification requires estimation of the T1 relaxation time of blood (T1<sub>b</sub>) (17). In these preterm infants, hematocrit level was regularly measured by using an automated analyzer (Sysmex XN-2000; Sysmex). For each preterm MRI scan, T1<sub>b</sub> was estimated from the hematocrit (Hct) value by using the following relationships:  $1/T1_b = 1.1 \text{ Hct} + 0.26$  at 1.5 T and  $1/T1_b = 0.5 \text{ Hct} + 0.37$  at 3.0 T (18,19). For those MRI scans for which a hematocrit measurement was not available, T1<sub>b</sub> was assumed to be the same as the average T1<sub>b</sub> value in the other infants for 1.5 T and 3.0 T separately. In all full-term infants, T1<sub>b</sub> was not available and was assumed to be 1810 msec for their scans at 3.0 T based on prior literature (8).

### Image Registration and Segmentation

CBF images were registered to anatomic images using the open-source rigid-body image registration algorithm of ANTs (version 1.9; University of Philadelphia) (20). Anatomic images were then automatically segmented using the open-source Draw-EM tool kit (version 2.0; Imperial College London) (21) to generate masks of the cortical gray matter (CGM), white matter (WM), deep gray matter (DGM), and cerebellum. These segmentations were reviewed for quality assurance and were further refined using manual correction. Global CBF was also calculated by merging all these regions into one.

### Classification of Brain Injury

A board-certified pediatric neuroradiologist (J.M., with 8 years of experience in pediatric neuroradiology) reviewed anatomic images acquired in preterm infants at TEA (ie, MRI 3) and assigned grades of brain injury at a rate of approximately one infant every 2 weeks. He was blinded to any other clinical indication for the examination beyond the need for MRI 3. Parenchymal abnormality was graded based on the Kidokoro et al scoring system as low-grade (normal or mild, score  $\leq 7$ ) or high-grade (moderate or severe, score  $>7$ ) injury (22). Intraventricular hemorrhage (IVH) was graded according to modified Papile classification as low-grade (none, grade I or II) or high-grade (grade III or IV) IVH (23). A random sample of 20 infants were rescored by the neuroradiologist after a

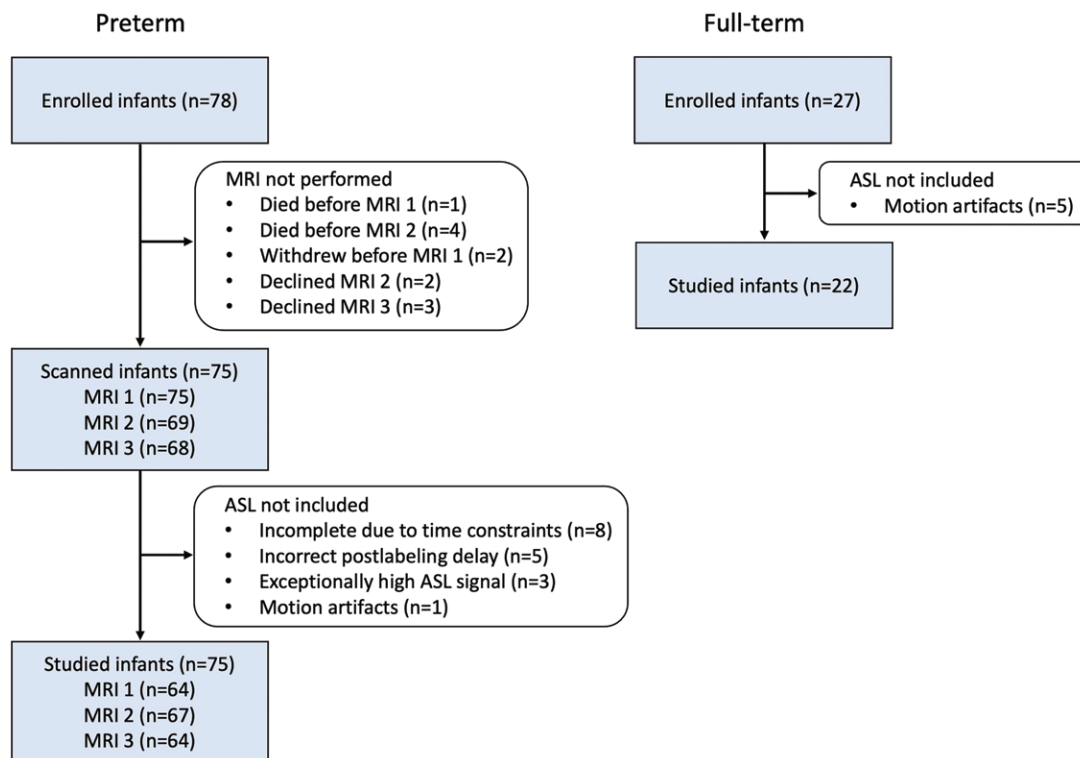


**Figure 1:** Flowchart of infant enrollment and data exclusion. ASL = arterial spin labeling.

6-month gap from the original reading to estimate reliability of the Kidokoro scoring.

### Association between CBF and Clinical Risk Factors

We investigated the relationship between regional and global CBF and clinical risk factors, including chorioamnionitis, sepsis, bronchopulmonary dysplasia, retinopathy of prematurity, steroid treatment, opioid treatment, sedative treatment, cardiac vasopressor support, length of oxygen support (in days), highest level of respiratory support (none, noninvasive, ventilator, or high-frequency oscillatory ventilation), treatment for necrotizing enterocolitis (no symptoms, medically managed [stage I or II], or surgically managed [mostly stage III, some stage II]), and treatment for patent ductus arteriosus (PDA) (no symptoms or undiagnosed, medically managed [including treatment with indomethacin {Indocin; Merck}], or surgically ligated).

### Statistical Analyses

Demographic and clinical characteristics of our preterm and full-term cohorts were compared using Mann-Whitney U test and Fisher exact test, as appropriate. Normality of all outcomes was confirmed prior to CBF analysis. Associations between mean CBF and PMA were assessed using generalized estimating equations to account for repeated measures in the same individual. Second-order polynomial models were tested using quadratic PMA terms; interaction terms with  $P < .10$  were explored further and reported if quasi-information criterion suggested better model fit. An unstructured covariance with sandwich variance estimates was assumed for all generalized estimating equation models based on best fit according to the quasi-information

criterion. Mean CBF was compared between different brain regions, low- and high-grade brain injury, and clinical risk factors, using least squares mean estimates from generalized estimating equation models controlling for PMA. Differences in mean CBF between preterm and full-term infants at TEA were evaluated using analysis of covariance adjusting for PMA. Tukey-Kramer  $P$  value adjustment method was applied to analyses to control for multiple comparisons. All analyses were performed with SAS software (version 9.4; SAS Institute); a  $P$  value of .05 was considered indicative of a significant difference.

## Results

### Study Population

Five of the 78 preterm infants died during the study, and seven families withdrew from the study or refused at least one of the three scans. Eight ASL scans were incomplete due to time constraints, and nine were excluded from our analysis. Of these nine scans, five were excluded due to an incorrect postlabeling delay (1 second), three were excluded due to exceptionally high ASL signal (global CBF  $>30$  mL/100 g/min) possibly caused by reconstruction failure of the scanner or infant motion coupled with background suppression failure, and one was excluded due to severe motion artifacts. As a result, a total of 195 ASL scans from 75 preterm infants (mean PMA: 29.5 weeks  $\pm$  2.3, 34.9 weeks  $\pm$  0.8, and 39.3 weeks  $\pm$  2.0 for MRI 1, 2, and 3, respectively; 43 male infants) were included in this study. Among the 27 healthy full-term infants enrolled for one MRI scan, five were excluded from our analysis because of severe motion artifacts; the remaining 22 healthy infants (mean

**Table 1: Perinatal Characteristics of the Study Cohort**

Perinatal Characteristic	Preterm Infants (n = 75)	Full-Term Infants (n = 22)	P Value
Birth GA (wk)	27.0 ± 2.5	38.7 ± 1.9	<.001
Birth weight (g)	1000 ± 325	3278 ± 535	<.001
Male sex*	43 (57)	13 (59)	.23
Ethnicity*	Black, 43; Hispanic, 10; White, 7; Other, 15	Black, 2; Hispanic, 2; White, 15; Other, 3	<.001
Apgar score at 1 minute	4.2 ± 2.2	7.7 ± 1.5	<.001
Apgar score at 5 minutes	6.7 ± 1.7	8.5 ± 0.9	<.001
Maternal age (y)	27.9 ± 5.6	36.2 ± 6.6	<.001
C-section delivery*	48 (64)	9 (41)	.08

Note.—Unless otherwise indicated, data are mean ± standard deviation, and data in parenthesis are percentages. GA = gestational age.  
\* Data are numbers of patients, and data in parentheses are percentages.

**Table 2: MRI Characteristics of the Study Cohort**

MRI Characteristic	Preterm Infants (n = 75)			Full-term Infants (n = 22)
	MRI 1 (n = 64)	MRI 2 (n = 67)	MRI 3 (n = 64)	
PMA at MRI (wk)	29.5 ± 2.3	34.9 ± 0.8	39.3 ± 2.0	42.1 ± 2.0
DOL at MRI (d)	17.4 ± 10.8	55.0 ± 16.9	84.1 ± 22.9	23.8 ± 14.7
Weight at MRI (g)	1109 ± 337	1887 ± 795	2698 ± 656	3547 ± 1421
Sedation at MRI*†	20 (31)	5 (7)	0 (0)	0 (0)
Supplemental oxygen at MRI†	58 (91)	45 (67)	22 (34)	0 (0)
Ventilator†	29	17	4	...
NIPPV†	11	5	0	...
CPAP†	9	5	1	...
NC†	8	17	17	...
Vapotherm†	1	1	0	...

Note.—Unless otherwise indicated, data are mean ± standard deviation. CPAP = continuous positive airway pressure, DOL = days of life, NC = nasal cannula, NIPPV = nasal intermittent positive pressure ventilation, PMA = postmenstrual age.

\* Sedation was all clinically indicated, not for MRI and was performed using morphine, midazolam, or fentanyl.

† Data are numbers of patients, and data in parenthesis are percentages.

PMA, 42.1 weeks ± 2.0; 13 male infants) were included. Figure 1 is a flowchart showing infant enrollment and data exclusion criteria. Tables 1 and 2 summarize the characteristics of the study cohorts. Among 64 preterm infants who underwent MRI 3, 49 had a low-grade parenchymal abnormality and 53 had low-grade IVH. Figure 2 shows examples of anatomic and ASL images in preterm infants with and those without brain injury. No structural abnormalities were found in the brain of healthy infants.

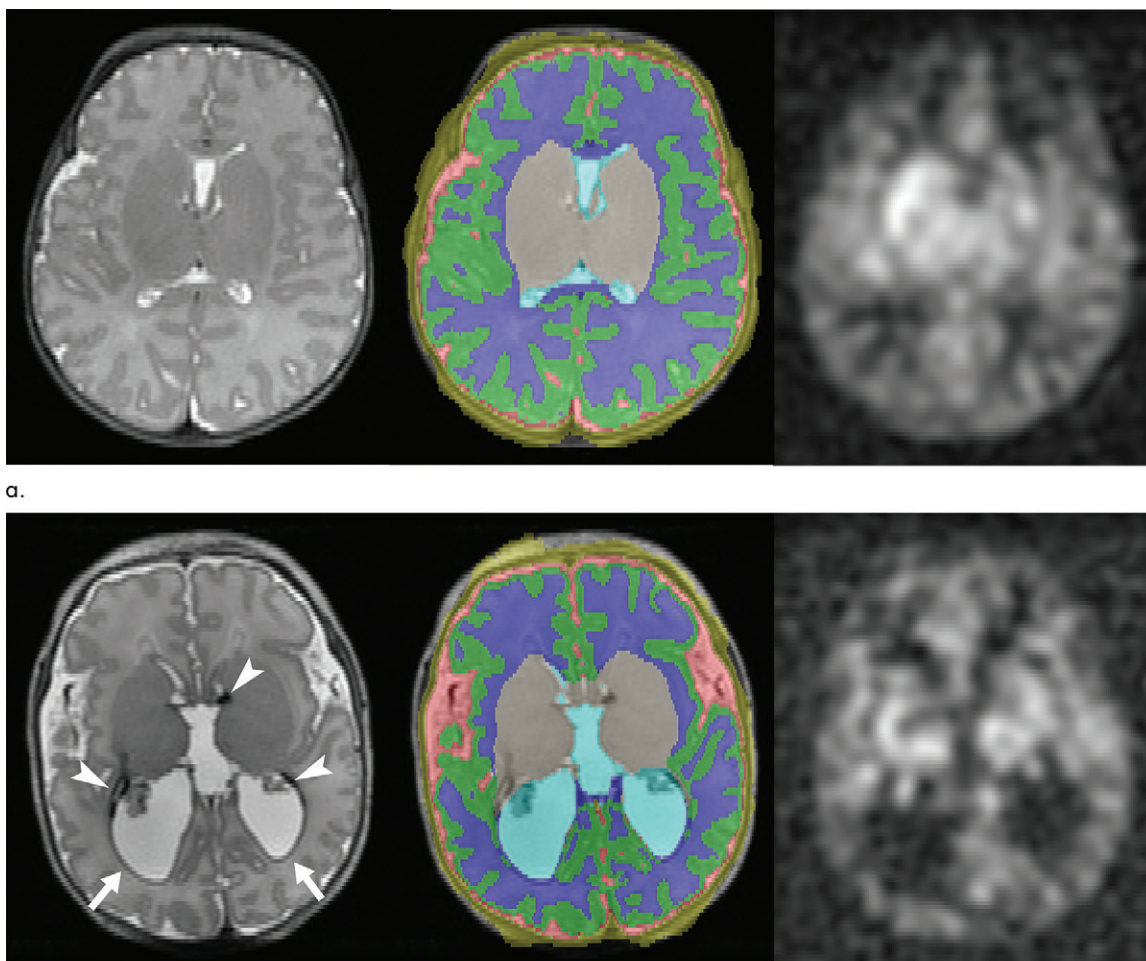
**Hematocrit Level and T1 of Blood**

Among 195 ASL scans, a hematocrit measurement was available for 181 scans. Mean hematocrit value was 34% ± 5 (range, 22%–47%) for PMA of 33.7 weeks ± 4.1 (range, 24.9–41.9 weeks), and the average time difference between MRI scanning and hematocrit measurement was 3 days ± 7. Average T1<sub>b</sub> value estimated from hematocrit measurements was 1586 msec ± 151 (range, 1287–1979 msec) for PMA of 31.8 msec ± 3.2 (range, 24.9–37.4 weeks) at 1.5 T and

1891 msec ± 70 (range, 1712–2026 msec) for PMA of 38.2 weeks ± 1.7 (range, 34.3–41.9 weeks) at 3.0 T. As expected, T1<sub>b</sub> was higher at 3.0 T because T1 is proportional to field strength. Scatter plots of hematocrit and T1<sub>b</sub> values as a function of PMA are shown in Figure 3a and 3b. Significant associations between hematocrit level and PMA (P < .001) and between T1<sub>b</sub> value and PMA were noted at 1.5 T (P = .003, nonlinear P = .002) but not at 3.0 T (P = .37). Regression equations are as follows: Hct = 48.0914–0.4327 PMA, T1<sub>b</sub> = 5726.869–285.252 PMA + 4.8252 PMA<sup>2</sup> at 1.5 T, and T1<sub>b</sub> = 1640.351 + 6.5813 PMA at 3.0 T. For CBF quantification of preterm scans where hematocrit measurement was not available, T1<sub>b</sub> values of 1586 msec at 1.5 T and 1891 msec at 3.0 T were used.

**1.5-T versus 3.0-T MRI**

Figure 3c shows global CBF measured at 1.5 T (123 scans) and 3.0 T (72 scans). Linear regression lines of mean CBF at the two field strengths show very similar trajectories: av-



a.

b.

**Figure 2:** Representative images of the preterm brain in infants **(a)** without brain injury and **(b)** with brain injury after segmentation and coregistration. Left: Anatomic images acquired with T2-weighted imaging show excellent contrast between different brain regions and brain injury, such as dilated ventricles (arrows) and intraventricular hemorrhage (arrowheads). Middle: Brain segmentation laid on anatomic images shows successful delineation of the brain regions (green, cortical gray matter; dark blue, white matter; gray, deep gray matter; light blue, ventricles; red, cerebrospinal fluid). Right: Arterial spin labeling images registered to the anatomic images show high-perfusion signal intensity, mostly in the gray matter.

erage CBF =  $0.0126 + 0.3454 \text{ PMA}$  at 1.5 T and  $-8.9059 + 0.5779 \text{ PMA}$  at 3.0 T. There was no significant difference in global CBF measurement between 1.5 T and 3.0 T when controlling for PMA ( $P = .76$ ), suggesting that data analysis with no distinction between the two field strengths may be reasonable.

#### Longitudinal Changes of Regional CBF

The averages of regional CBF in all preterm infants are summarized in Table 3. There were significant differences in mean CBF between all regions (all  $P < .001$ ). Figure 4 shows temporal changes in regional CBF. Regional CBF significantly increased with advancing PMA in all regions. Nonlinear associations between mean CBF and PMA were noted for WM and the cerebellum. The cerebellum showed both the highest mean CBF and the most rapid increase (based on  $\beta$ ) in mean CBF. Regression equations of average CBF are as follows:  $\text{CBF}_{\text{CGM}} = 7.6582 + 0.1695 \text{ PMA}$  ( $P = .02$ ),  $\text{CBF}_{\text{WM}} = 15.3864 - 0.7742 \text{ PMA} + 0.0172 \text{ PMA}^2$  ( $P < .001$ , linear  $\beta = 0.39$ ),  $\text{CBF}_{\text{DGM}} = 1.6488 + 0.4456 \text{ PMA}$  ( $P < .001$ ),  $\text{CBF}_{\text{cerebellum}} = -38.6069 + 2.7895 \text{ PMA} - 0.0321 \text{ PMA}^2$  ( $P < .001$ , linear  $\beta = 0.61$ ), and  $\text{CBF}_{\text{global}} = -1.0102 + 0.3759 \text{ PMA}$  ( $P < .001$ ).

$P < .001$ , linear  $\beta = 0.39$ ),  $\text{CBF}_{\text{DGM}} = 1.6488 + 0.4456 \text{ PMA}$  ( $P < .001$ ),  $\text{CBF}_{\text{cerebellum}} = -38.6069 + 2.7895 \text{ PMA} - 0.0321 \text{ PMA}^2$  ( $P < .001$ , linear  $\beta = 0.61$ ), and  $\text{CBF}_{\text{global}} = -1.0102 + 0.3759 \text{ PMA}$  ( $P < .001$ ).

#### Association between CBF and Brain Injury

The averages of regional CBF in preterm infants with low- or high-grade parenchymal abnormality or low- or high-grade IVH and associated  $P$  values are listed in Table 3. There were no significant differences in regional mean CBF between low- and high-grade parenchymal abnormality groups (all  $P > .6$ ). In contrast, mean CBF was noted to be lower in preterm infants with high-grade IVH in all regions compared with those with low-grade IVH (all  $P \leq .05$ ). Temporal changes of regional CBF in these subgroups are shown in Figure 5. Intrarater reliability was high for Kidokoro scores (weighted  $\kappa$ , 0.86; 95% CI: 0.75, 0.97). This degree of concordance resulted in perfect agreement of dichotomized scores (Cohen  $\kappa$ , 1.00).

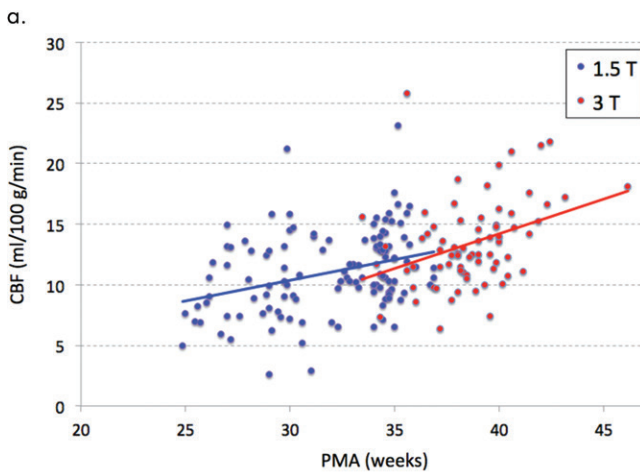
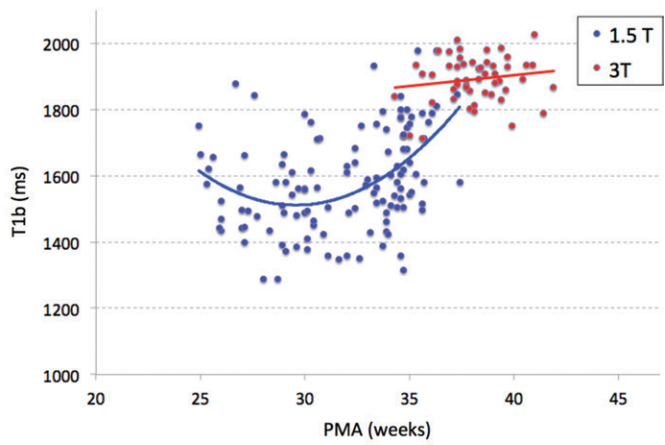
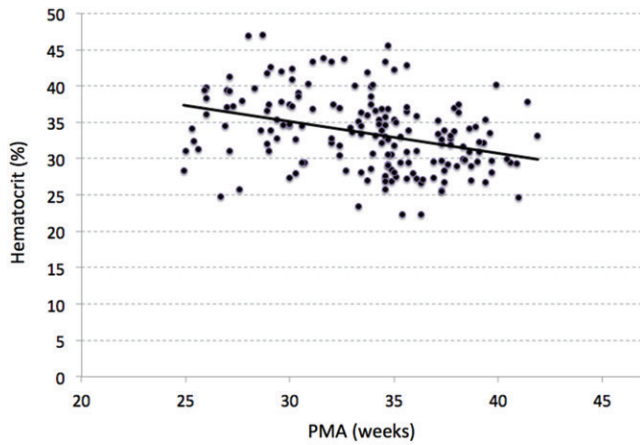


**Figure 3:** (a) Scatter plot shows hematocrit level measured in preterm infants. (b) Scatter plot shows T1 relaxation time of blood (T1<sub>b</sub>) estimated from hematocrit measurement at either 1.5 T or 3.0 T depending on MRI field strength. Postmenstrual age (PMA) indicates PMA at hematocrit measurement rather than PMA at MRI. (c) Scatter plot shows global cerebral blood flow (CBF) in preterm infants quantified by using estimated T1<sub>b</sub>. There was no significant difference in mean CBF between the two field strengths when controlling for PMA. Regression lines were calculated using generalized estimating equation models to accommodate repeated measures from the same infant. A second-order polynomial was included in the T1<sub>b</sub> model at 1.5 T due to the significance of the quadratic term at  $P < .10$ , whereas the other regression lines were linear.

**Table 3: CBF Measurements in Preterm and Full-term Infants**

ROI	Preterm							TEA Scan (mL/100 g/min)	Full-Term Infants (mL/100 g/min)	P Value
	PA			IVH						
	All (mL/100 g/min)	Low (mL/100 g/min)	High (mL/100 g/min)	P Value	Low (mL/100 g/min)	High (mL/100 g/min)	P Value			
CGM	13.5 ± 0.3	13.5 ± 0.3	13.8 ± 0.7	.69	13.8 ± 0.3	12.5 ± 0.7	.05	14.7 ± 0.4	12.2 ± 0.7	.007
WM	9.4 ± 0.2	9.5 ± 0.2	9.6 ± 0.5	.88	9.7 ± 0.2	8.7 ± 0.4	.01	11.8 ± 0.3	10.1 ± 0.6	.02
DGM	17.0 ± 0.4	17.2 ± 0.4	17.0 ± 1.0	.87	17.6 ± 0.4	15.3 ± 0.8	.01	19.4 ± 0.6	15.2 ± 1.2	.003
Cerebellum	18.8 ± 0.5	19.0 ± 0.5	19.9 ± 1.6	.96	19.5 ± 0.6	16.8 ± 1.3	.05	21.3 ± 0.7	15.7 ± 1.3	<.001
Global	11.9 ± 0.2	12.0 ± 0.3	12.2 ± 0.6	.76	12.3 ± 0.3	11.0 ± 0.4	.009	14.2 ± 0.4	11.7 ± 0.7	.006

Note.—Data are mean ± standard error. CGM = cortical gray matter, DGM = deep gray matter, IVH = intraventricular hemorrhage, PA = parenchymal abnormality, ROI = region of interest, TEA = term-equivalent age, WM = white matter.

**Preterm at TEA versus Full-term Infants**

Preterm infants at TEA showed significantly higher mean CBF in all regions compared with full-term infants, as shown in Table 3 and Figure 6 (all  $P \leq .02$ ). However, when comparing preterm infants with high-grade IVH and full-term infants, no significant differences in mean CBF were

found, except in the cerebellum, where a marginal difference was noted ( $P = .05$ ). When comparing CBF from scans acquired within a predefined TEA period (range, 37–42 weeks PMA), which is a subset of all TEA scans (range: 35 weeks 6 days to 46 weeks 1 day PMA), no significant differences in mean CBF were observed between preterm and

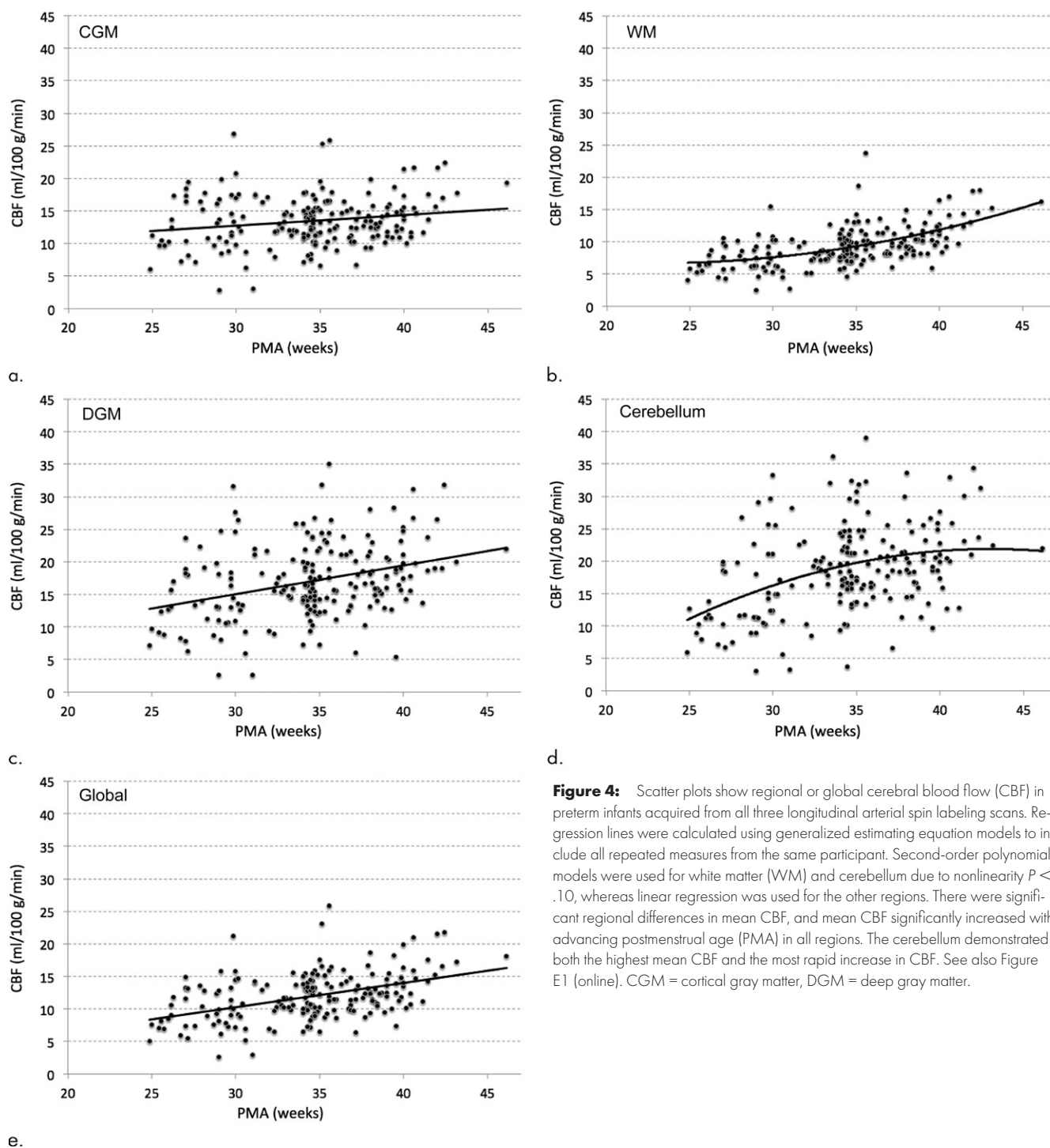


**Figure 4:** Scatter plots show regional or global cerebral blood flow (CBF) in preterm infants acquired from all three longitudinal arterial spin labeling scans. Regression lines were calculated using generalized estimating equation models to include all repeated measures from the same participant. Second-order polynomial models were used for white matter (WM) and cerebellum due to nonlinearity  $P < .10$ , whereas linear regression was used for the other regions. There were significant regional differences in mean CBF, and mean CBF significantly increased with advancing postmenstrual age (PMA) in all regions. The cerebellum demonstrated both the highest mean CBF and the most rapid increase in CBF. See also Figure E1 (online). CGM = cortical gray matter, DGM = deep gray matter.

full-term infants, except in the cerebellum ( $P = .02$ ), where full-term CBF remained lower.

#### Association between CBF and Clinical Risk Factors

Among all clinical risk factors examined, only PDA was significantly associated with mean CBF in preterm infants. The averages of regional CBF in different preterm infant groups stratified by PDA are included in Table 4. Preterm infants with medically managed PDA had lower regional CBF in the WM and DGM (both  $P = .03$ ) compared with preterm

infants without PDA. There was no significant difference in mean CBF between preterm infants with surgically ligated PDA treatment and those without PDA (all  $P > .5$ ).

#### Discussion

We report that serial third-trimester cerebral blood flow (CBF) increased significantly in all brain regions with advancing postmenstrual age (PMA), with the cerebellum exhibiting both the highest mean and the most rapid increase of CBF. We also demonstrate that CBF was associated with intraventricular



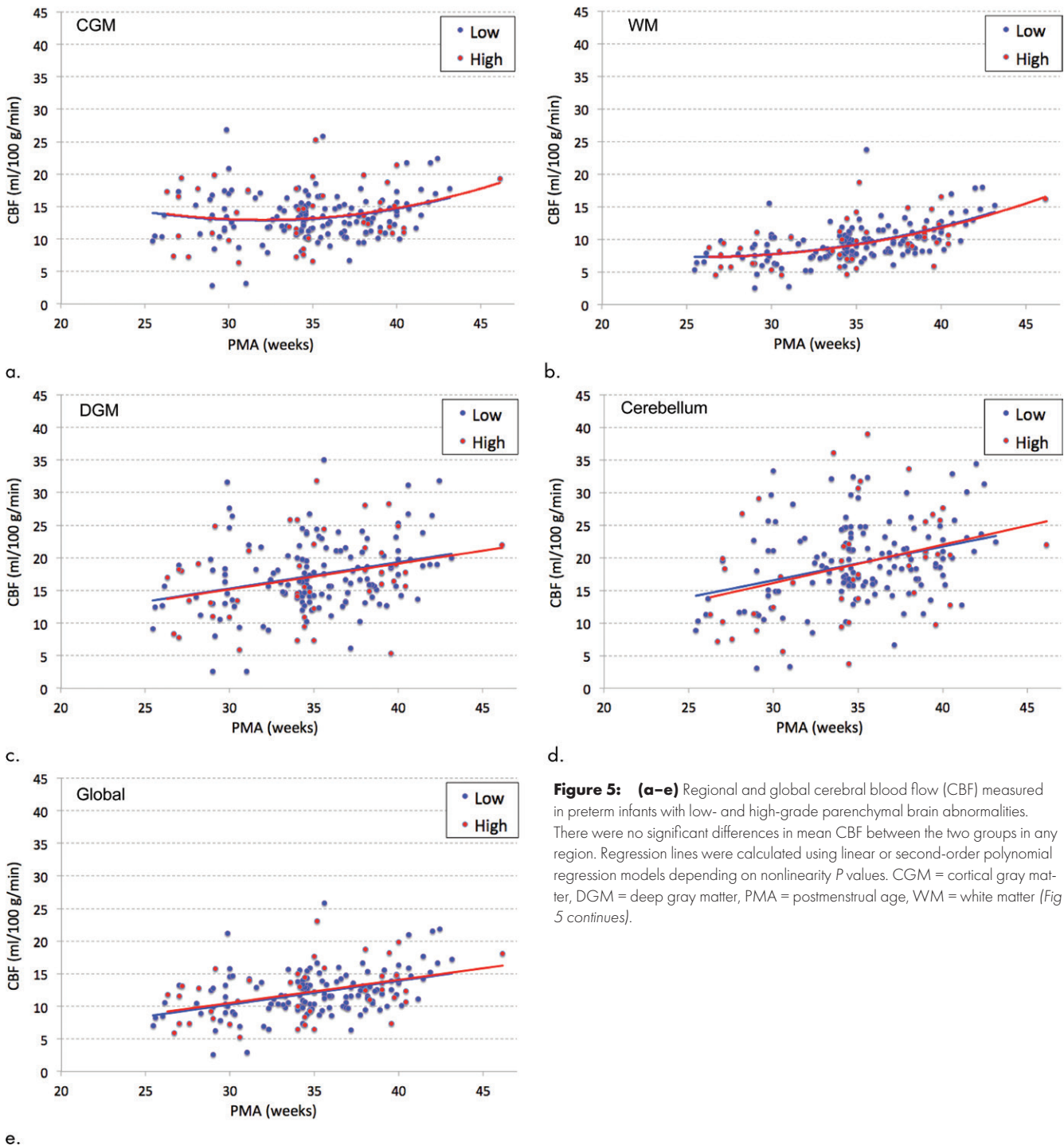


**Figure 5:** (a–e) Regional and global cerebral blood flow (CBF) measured in preterm infants with low- and high-grade parenchymal brain abnormalities. There were no significant differences in mean CBF between the two groups in any region. Regression lines were calculated using linear or second-order polynomial regression models depending on nonlinearity *P* values. CGM = cortical gray matter, DGM = deep gray matter, PMA = postmenstrual age, WM = white matter (Fig 5 continues).

hemorrhage and patent ductus arteriosus (PDA) and was higher in preterm infants at term-equivalent age (TEA) than in full-term control infants.

When ASL is applied to newborns, there are several pitfalls in selecting parameters for data acquisition and data analysis. First, postlabeling delay must be increased compared with that in children or young adults because of slower blood velocity in the newborn brain (24,25). Second,  $T_{1b}$  needs to be measured in each infant for accurate quantification because  $T_{1b}$  of newborns is different from that of adults and because there is a

wide variation across different infants and different ages (19). Last, while many preterm ASL studies used small regions of interest drawn manually on a few slices (6,7,11,13–15), larger regions of interest may be desirable for increased confidence in ASL measurements through massive signal averaging within each region (26). In this study, we addressed these obstacles to acquire reliable measurements of regional CBF in newborn infants. Measurement of exact arterial transit delay in newborns may be warranted in future studies to confirm optimal postlabeling delay.

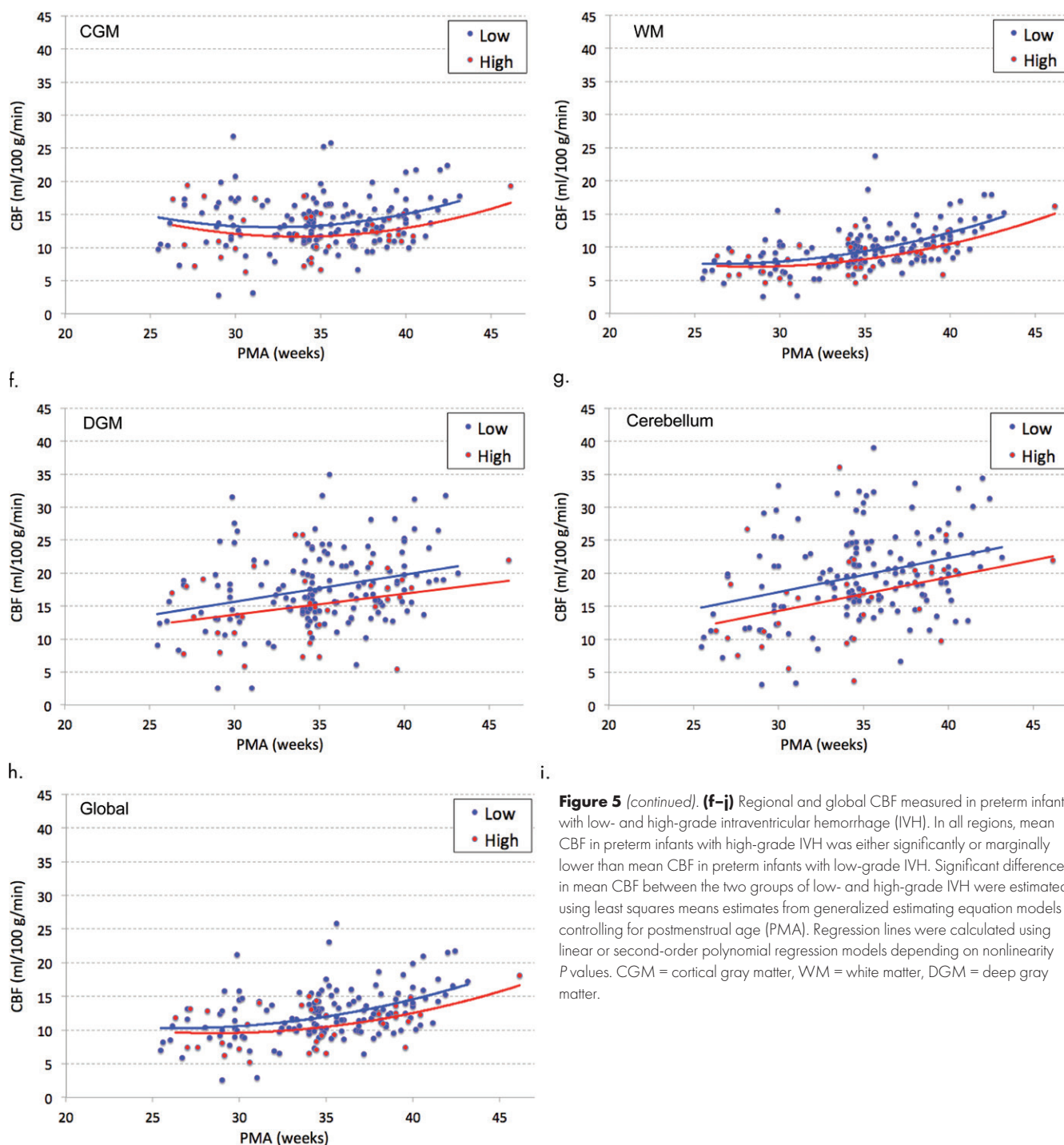
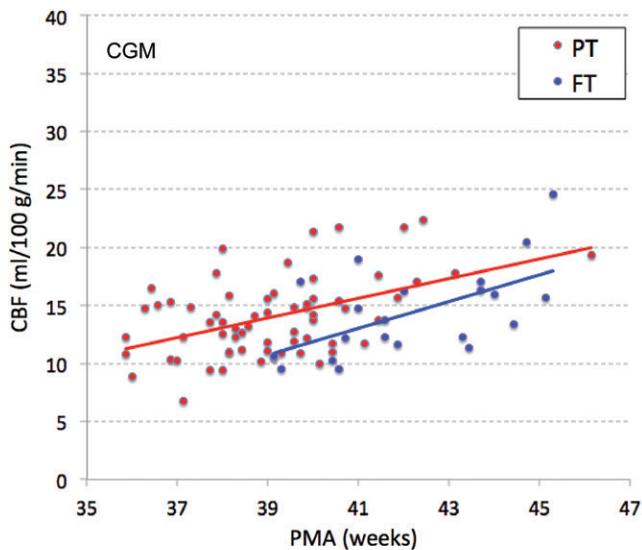


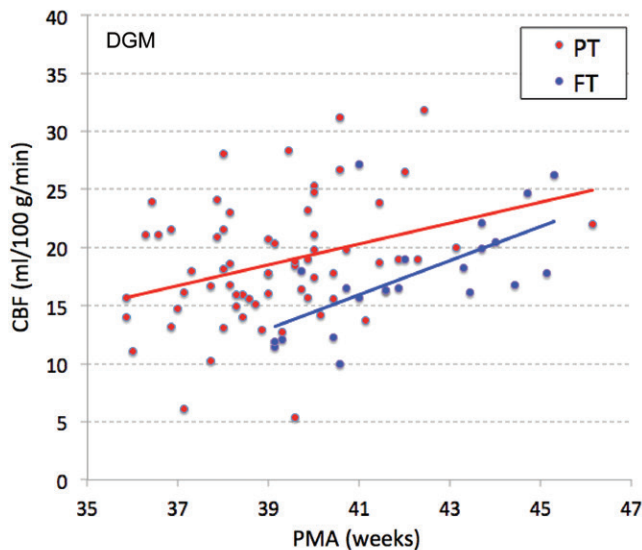
**Figure 5** (continued). (f–j) Regional and global CBF measured in preterm infants with low- and high-grade intraventricular hemorrhage (IVH). In all regions, mean CBF in preterm infants with high-grade IVH was either significantly or marginally lower than mean CBF in preterm infants with low-grade IVH. Significant differences in mean CBF between the two groups of low- and high-grade IVH were estimated using least squares means estimates from generalized estimating equation models controlling for postmenstrual age (PMA). Regression lines were calculated using linear or second-order polynomial regression models depending on nonlinearity  $P$  values. CGM = cortical gray matter, WM = white matter, DGM = deep gray matter.

Our quantified global CBF measurements in preterm infants are largely in agreement with previous preterm ASL studies (6–9,12–15). Our measurements are most comparable to those in the studies by De Vis et al (7–9), in which  $T1_b$  was measured in each infant, similar to our study. Our measurements also showed good agreement with preterm studies of other imaging modalities, such as PET (27), near-infrared spectroscopy (28), xenon clearance technique (29), and US (30). Among these, our measurements showed the best agreement with the study based on PET (mean CBF of 11.6 mL/100 g/min at 32 weeks), which is the reference standard for CBF measurements in humans.

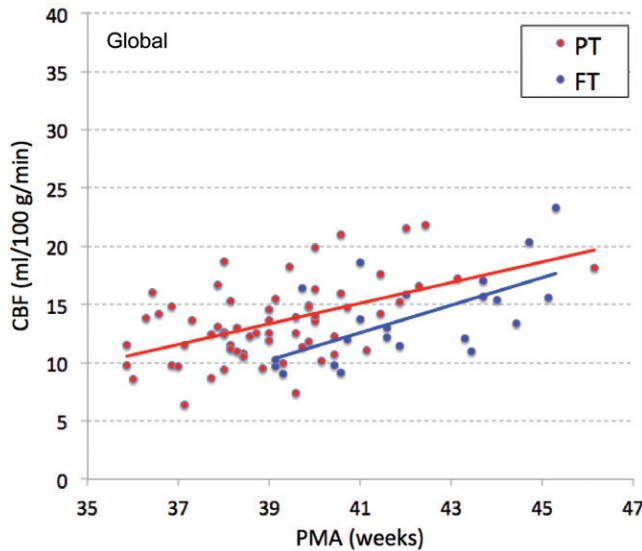
Our longitudinal analysis of preterm infants demonstrated that mean CBF significantly increased with advancing PMA in all regions during the third trimester, likely reflecting accelerated brain development and increasing metabolic demand for blood-borne oxygen and nutrients in this critical period. Also, mean CBF was significantly different across brain regions, being highest in the cerebellum, followed by DGM, CGM, and WM. To our knowledge, no previous studies have measured CBF in



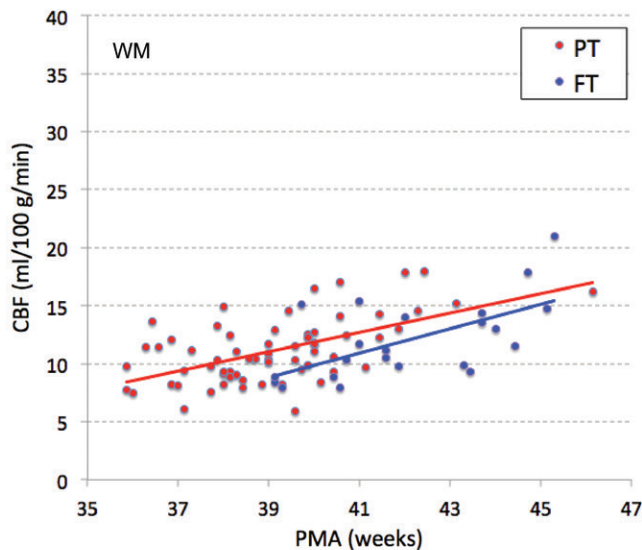
a.



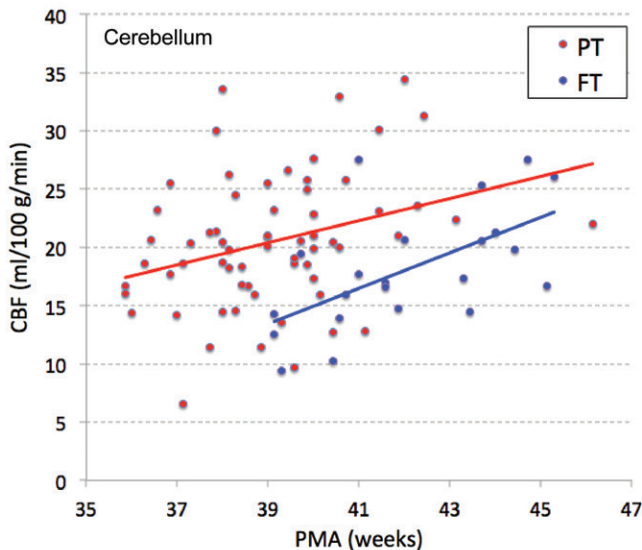
c.



e.



b.



d.

**Figure 6:** Scatter plots show comparison of regional and global cerebral blood flow (CBF) measured in preterm infants at term-equivalent age and in full-term infants. Mean CBF of full-term infants was significantly lower than that of preterm infants in all regions based on analysis of covariance models adjusting for postmenstrual age (PMA). CGM = cortical gray matter, DGM = deep gray matter, FT = full-term, PT = preterm, WM = white matter.

**Table 4: CBF Measurements in Preterm Infant Groups Stratified by PDA**

ROI	No Symptoms (mL/100 g/min)	Medically Managed PDA (mL/100 g/min)	Surgically Ligated PDA (mL/100 g/min)
CGM	13.7 ± 0.3	12.8 ± 0.4 (.21)	14.1 ± 0.7 (.88)
WM	9.6 ± 0.2	8.8 ± 0.3 (.03)	9.9 ± 0.5 (.54)
DGM	17.6 ± 0.5	15.6 ± 0.6 (.03)	17.7 ± 0.9 (.94)
Cerebellum	19.3 ± 0.7	17.3 ± 0.9 (.17)	19.7 ± 1.0 (.94)
Global	12.2 ± 0.3	11.2 ± 0.3 (.06)	12.5 ± 0.6 (.88)

Note.—Unless otherwise indicated, data are mean ± standard error. Data in parentheses are *P* values and are for comparison with infants with no symptoms. CGM = cortical gray matter, DGM = deep gray matter, PDA = patent ductus arteriosus, ROI = region of interest, WM = white matter.

the cerebellum. However, it has been shown that the cerebellum has the most rapid volumetric growth during the third trimester in both healthy fetuses and preterm infants (3,31), which is in line with our CBF results in the present study.

We report a significant association between CBF and IVH in preterm infants. Previous studies also demonstrated associations between brain injury and low ASL CBF (12–14) or low oxygen delivery based on results of near-infrared spectroscopy (32,33). Particularly, one study showed that oxygen delivery in the preterm brain was associated with IVH but not parenchymal injury (32). Another study demonstrated that lower cerebral oxygenation in the preterm brain was associated with higher-grade IVH, while cerebral oxygenation was not affected by fetal inflammation, which increases the risk of parenchymal WM injury (33). It has been suggested that development of IVH may be associated with fluctuating blood flow or reduced arterial blood pressure (34).

Mean CBF was significantly higher in preterm infants than in full-term infants in the present study, which is consistent with the results of previous preterm ASL studies (6,10,12,13). Higher postnatal age of preterm infants has been suggested to be responsible for higher CBF (6,12,13), presumably as a result of longer exposure to the extrauterine environment, which advances brain development (35).

Interestingly, infants with ligated PDA showed no difference in mean CBF compared with infants without PDA, whereas infants with medically managed PDA showed significantly reduced mean CBF. This may be related to the fact that PDA ligation was mostly performed before MRI 1 or MRI 2 in our protocol; thus, CBF was possibly restored by the time of MRI. Further studies with concurrent assessments of ductus arteriosus and CBF are needed to better address the mechanisms underlying this important association.

This study had limitations. First, the field strength we used was heterogeneous. While full-term scans were performed at 3.0 T for enhanced signal-to-noise ratio, early preterm scans had to be performed at 1.5 T because the lower patient weight would increase specific absorption rate. However, we carefully determined relaxation times for quantification and confirmed there were no significant differences in mean CBF between the two field strengths. Second, the current labeling efficiency of pseudocontinuous ASL may not be optimal for preterm infants. The default parameters of pseudocontinuous labeling pulses are

optimized for blood velocity in the adult carotid arteries, and labeling efficiency may diminish with slower blood flow in the newborn brain (16).

We report the longitudinal trajectories of regional cerebral blood flow (CBF) in preterm infants across the ex utero third trimester. Regional CBF in all areas increased significantly with advancing postmenstrual age, with the cerebellum showing the most rapid increase and highest

mean CBF during this period. Lower CBF was associated with intraventricular hemorrhage but not parenchymal abnormalities. Lower CBF also was associated with medically managed patent ductus arteriosus (PDA) but not ligated PDA. Future work should assess the relationship between CBF trajectories and long-term neurodevelopment outcomes in infants undergoing ex utero brain development across the third trimester, to demonstrate that CBF measurement may be used as an early biomarker for neurodevelopmental impairments in this high-risk population.

**Acknowledgments:** The authors thank the families who participated in this study.

**Author contributions:** Guarantors of integrity of entire study, Z.Z., C.L.; study concepts/study design or data acquisition or data analysis/interpretation, all authors; manuscript drafting or manuscript revision for important intellectual content, all authors; approval of final version of submitted manuscript, all authors; agrees to ensure any questions related to the work are appropriately resolved, all authors; literature research, Z.Z., K.K., S.B., C.L.; clinical studies, Z.Z., S.B., N.A., T.C., A.d.P., C.L.; statistical analysis, Z.Z., M.J.; and manuscript editing, Z.Z., M.J., S.B., M.S., N.A., J.M., T.C., A.d.P., C.L.

**Disclosures of Conflicts of Interest:** Z.Z. disclosed no relevant relationships. K.K. disclosed no relevant relationships. M.J. Activities related to the present article: disclosed no relevant relationships. Activities not related to the present article: institution received grants from Pfizer. Other relationships: disclosed no relevant relationships. S.B. disclosed no relevant relationships. M.S. disclosed no relevant relationships. N.A. disclosed no relevant relationships. J.M. Activities related to the present article: disclosed no relevant relationships. Activities not related to the present article: provided expert testimony for Slattery Petersen; the U.S. Attorney, Northern District of Illinois; and Kilgore & Smith. Other relationships: disclosed no relevant relationships. T.C. disclosed no relevant relationships. A.d.P. disclosed no relevant relationships. C.L. disclosed no relevant relationships.

## References

- Volpe JJ. Brain injury in premature infants: a complex amalgam of destructive and developmental disturbances. *Lancet Neurol* 2009;8(1):110–124.
- Scott JA, Habas PA, Kim K, et al. Growth trajectories of the human fetal brain tissues estimated from 3D reconstructed in utero MRI. *Int J Dev Neurosci* 2011;29(5):529–536.
- Andescavage NN, du Plessis A, McCarter R, et al. Complex Trajectories of Brain Development in the Healthy Human Fetus. *Cereb Cortex* 2017;27(11):5274–5283.
- Detre JA, Leigh JS, Williams DS, Koretsky AP. Perfusion imaging. *Magn Reson Med* 1992;23(1):37–45.
- Williams DS, Detre JA, Leigh JS, Koretsky AP. Magnetic resonance imaging of perfusion using spin inversion of arterial water. *Proc Natl Acad Sci U S A* 1992;89(1):212–216.
- Miranda MJ, Olofsson K, Sidaros K. Noninvasive measurements of regional cerebral perfusion in preterm and term neonates by magnetic resonance arterial spin labeling. *Pediatr Res* 2006;60(3):359–363.
- De Vis JB, Petersen ET, de Vries LS, et al. Regional changes in brain perfusion during brain maturation measured non-invasively with Arterial Spin Labeling MRI in neonates. *Eur J Radiol* 2013;82(3):538–543.

8. De Vis JB, Hendrikse J, Groenendaal F, et al. Impact of neonate haematocrit variability on the longitudinal relaxation time of blood: Implications for arterial spin labelling MRI. *Neuroimage Clin* 2014;4:517–525.
9. De Vis JB, Petersen ET, Alderliesten T, et al. Non-invasive MRI measurements of venous oxygenation, oxygen extraction fraction and oxygen consumption in neonates. *Neuroimage* 2014;95:185–192.
10. Wintermark P, Lechpammer M, Kosaras B, Jensen FE, Warfield SK. Brain Perfusion Is Increased at Term in the White Matter of Very Preterm Newborns and Newborns with Congenital Heart Disease: Does this Reflect Activated Angiogenesis? *Neuropediatrics* 2015;46(5):344–351.
11. Ouyang M, Liu P, Jeon T, et al. Heterogeneous increases of regional cerebral blood flow during preterm brain development: Preliminary assessment with pseudo-continuous arterial spin labeled perfusion MRI. *Neuroimage* 2017;147:233–242.
12. Tortora D, Mattei PA, Navarra R, et al. Prematurity and brain perfusion: Arterial spin labeling MRI. *Neuroimage Clin* 2017;15:401–407.
13. Bouyssi-Kobar M, Murnick J, Brossard-Racine M, et al. Altered Cerebral Perfusion in Infants Born Preterm Compared with Infants Born Full Term. *J Pediatr* 2018;193:54–61.e2.
14. Mahdi ES, Bouyssi-Kobar M, Jacobs MB, Murnick J, Chang T, Limperopoulos C. Cerebral Perfusion Is Perturbed by Preterm Birth and Brain Injury. *AJNR Am J Neuroradiol* 2018;39(7):1330–1335.
15. Kim HG, Lee JH, Choi JW, Han M, Gho SM, Moon Y. Multidelay Arterial Spin-Labeling MRI in Neonates and Infants: Cerebral Perfusion Changes during Brain Maturation. *AJNR Am J Neuroradiol* 2018;39(10):1912–1918.
16. Dai W, Garcia D, de Bazelaire C, Alsop DC. Continuous flow-driven inversion for arterial spin labeling using pulsed radio frequency and gradient fields. *Magn Reson Med* 2008;60(6):1488–1497.
17. Buxton RB, Frank LR, Wong EC, Siewert B, Warach S, Edelman RR. A general kinetic model for quantitative perfusion imaging with arterial spin labeling. *Magn Reson Med* 1998;40(3):383–396.
18. Spees WM, Yablonskiy DA, Oswood MC, Ackerman JJ. Water proton MR properties of human blood at 1.5 Tesla: magnetic susceptibility,  $T_1^{(1)}$ ,  $T_1^{(2)}$ ,  $T_1^*$ , and non-Lorentzian signal behavior. *Magn Reson Med* 2001;45(4):533–542.
19. Varela M, Hajnal JV, Petersen ET, Golay X, Merchant N, Larkman DJ. A method for rapid in vivo measurement of blood T1. *NMR Biomed* 2011;24(1):80–88.
20. Avants BB, Tustison N, Song G. Advanced normalization tools (ANTS). *Insight J* 2009;2:1–35. <https://www.insight-journal.org/browse/publication/681>.
21. Makropoulos A, Gousias IS, Ledig C, et al. Automatic whole brain MRI segmentation of the developing neonatal brain. *IEEE Trans Med Imaging* 2014;33(9):1818–1831.
22. Kidokoro H, Neil JJ, Inder TE. New MR imaging assessment tool to define brain abnormalities in very preterm infants at term. *AJNR Am J Neuroradiol* 2013;34(11):2208–2214.
23. Papile LA, Burstein J, Burstein R, Koffler H. Incidence and evolution of subependymal and intraventricular hemorrhage: a study of infants with birth weights less than 1,500 gm. *J Pediatr* 1978;92(4):529–534.
24. Varela M, Groves AM, Arichi T, Hajnal JV. Mean cerebral blood flow measurements using phase contrast MRI in the first year of life. *NMR Biomed* 2012;25(9):1063–1072.
25. Alsop DC, Detre JA, Golay X, et al. Recommended implementation of arterial spin-labeled perfusion MRI for clinical applications: A consensus of the ISMRM perfusion study group and the European consortium for ASL in dementia. *Magn Reson Med* 2015;73(1):102–116.
26. Zun Z, Wong EC, Nayak KS. Assessment of myocardial blood flow (MBF) in humans using arterial spin labeling (ASL): feasibility and noise analysis. *Magn Reson Med* 2009;62(4):975–983.
27. Altman DI, Powers WJ, Perlman JM, Herscovitch P, Volpe SL, Volpe JJ. Cerebral blood flow requirement for brain viability in newborn infants is lower than in adults. *Ann Neurol* 1988;24(2):218–226.
28. Edwards AD, Wyatt JS, Richardson C, Delpy DT, Cope M, Reynolds EO. Cotside measurement of cerebral blood flow in ill newborn infants by near infrared spectroscopy. *Lancet* 1988;2(8614):770–771.
29. Greisen G. Cerebral blood flow in preterm infants during the first week of life. *Acta Paediatr Scand* 1986;75(1):43–51.
30. Kehler M, Krägeloh-Mann I, Goelz R, Schöning M. The development of cerebral perfusion in healthy preterm and term neonates. *Neuropediatrics* 2003;34(6):281–286.
31. Limperopoulos C, Soul JS, Gauvreau K, et al. Late gestation cerebellar growth is rapid and impeded by premature birth. *Pediatrics* 2005;115(3):688–695.
32. Kissack CM, Garr R, Wardle SP, Weindling AM. Postnatal changes in cerebral oxygen extraction in the preterm infant are associated with intraventricular hemorrhage and hemorrhagic parenchymal infarction but not periventricular leukomalacia. *Pediatr Res* 2004;56(1):111–116.
33. Sorensen LC, Maroun LL, Borch K, Lou HC, Greisen G. Neonatal cerebral oxygenation is not linked to foetal vasculitis and predicts intraventricular haemorrhage in preterm infants. *Acta Paediatr* 2008;97(11):1529–1534.
34. Perlman JM, McMenamin JB, Volpe JJ. Fluctuating cerebral blood-flow velocity in respiratory-distress syndrome. Relation to the development of intraventricular hemorrhage. *N Engl J Med* 1983;309(4):204–209.
35. Jandó G, Mikó-Baráth E, Markó K, Hollódy K, Török B, Kovacs I. Early-onset binocularity in preterm infants reveals experience-dependent visual development in humans. *Proc Natl Acad Sci U S A* 2012;109(27):11049–11052.